COMPUTATIONAL CONTINUUM MECHANICS

ВЫЧИСЛИТЕЛЬНАЯ МЕХАНИКА СЛОШНЫХ СРЕД

Computational Continuum Mechanics. 2021. Vol. 14. No. 3. pp. 264-277 DOI: 10.7242/1999-6691/2021.14.3.22

INFLUENCE OF THE INTERPARTICLE INTERACTION OF THE ENSEMBLE OF IMMOBILIZED SUPERPARAMAGNETIC FERROPARTICLES ON THE STATIC, MAGNETIC AND THERMODYNAMIC PROPERTIES OF THE SYSTEM

S.A. Sokolsky

Ural Mathematical Center, Ural Federal University, Ekaterinburg, Russian Federation

The paper presents a study of the effect of the interparticle dipole-dipole interaction on the static, thermodynamic, and magnetic properties of the ensemble of stationary superparamagnetic particles in the external magnetic field. The relaxation of the magnetic moment of the model ferroparticles occurred by the Néel mechanism. The directions of the easy axes of all particles were assumed to be parallel to each other, but at the angle to the direction of the external magnetic field. The direction of the easy axes was described using the polar and azimuth angles. The potential energy of the system includes a single-particle dipole-axial interaction, a single-particle dipole-field interaction, and long-range interparticle dipole-dipole correlations. In the system, two variants of the distribution of ferroparticles over the volume of the container are considered: at the nodes of a simple cubic lattice and randomly. The described model is studied theoretically by expanding the Helmholtz free energy into a classical virial series up to the second virial coefficient. Using the new theory, contribution of dipole-dipole interactions in the changes in the magnetic susceptibility, magnetization, and heat capacity of the system is estimated, and the results are represented graphically. The important information necessary to the development and synthesis of new magnetic materials with controlled properties is provided.

Key words: superparamagnetic particles, Helmholtz free energy, virial expansion, Mayer series, magnetization, initial susceptibility, heat capacity

1. Introduction

Smart materials are special materials having one or more properties that can be significantly changed by an external influence, for example, by a magnetic field. Such materials include magnetic composites, which are obtained by embedding magnetic nanoparticles into a liquid or polymer matrix. Examples of such composites are ferrofluids, ferrogels, magnetic elastomers, magnetic emulsions and various biocompatible magnetic fillers. Today, such materials are frequently used in the medicine because they actively react to applied magnetic fields. For instance, they are an essential tool for magnetic hyperthermia, in which the remagnetization of magnetic nanoparticles in an alternating magnetic field leads to the death of tumor cells. The response of magnetic composites to an applied magnetic field in nanoscale particles is determined by two main physical mechanisms of orientation relaxation of the magnetic moment: Brownian rotation of particles with fixed magnetic moments and superparamagnetic Néel rotation of magnetic moments inside particles due to thermal fluctuations. In ensembles of nanoparticles placed in certain liquid carriers, known as ferrofluids, both mechanisms take place. The introduction of nanoparticles in a polymer matrix or biological tissues leads to the loss of both translational and orientation freedom. In this case, superparamagnetic Néel relaxation becomes the main mechanism determining the magnetic properties of ensembles of such stationary nanoparticles.

Today, there are many well-established synthesis methods that make it possible to produce a magnetic composite with a variety of nano- and microscopic textures. The different distribution of magnetic nanoparticles inside the sample leads to a significant change in its bulk properties. In addition, interparticle dipole-dipole interactions have a strong effect on the macroproperties of the system, and this manifests itself differently in liquid or polymer-based composites. Thus, strong interparticle dipole-dipole interactions in a ferrofluid lead to aggregation [1-4], whereas in a system of stationary magnetic nanoparticles, interparticle interactions can only be the reason for structuring the magnetic moments of nanoparticles, since the particles themselves remain stationary [5-7]. The effect of dipole-dipole interactions on the bulk properties of ferrofluids has been well studied theoretically [8-12], experimentally [4, 13-15], and using computer modeling methods [4, 9-12, 16]. However, the development of a theory that takes into account dipole-dipole interactions in a system of stationary superparamagnetic nanoparticles still remains a difficult task. In recent works, the magnetic response of a system of stationary interacting single-domain nanoparticles distributed randomly or

Email addresses for correspondence: Sokolsky2304@gmail.com

placed at the nodes of a simple cubic lattice inside an implicit solid matrix has been studied using statistical-mechanical theory and computer modeling. In [17], superparamagnetic particles with uniaxial magnetic anisotropy were considered. The relaxation of the magnetic moments of the particles occurred by the Néel mechanism. The easy axes were arranged according to certain textures: aligned parallel or perpendicular to the external magnetic field, or occupied a random place. It has been established that the initial magnetic susceptibility of magnetic materials with different textures strongly depends on the magnetic anisotropy energy of the crystal, measured in units of thermal energy. All cases of interaction between nanoparticles led to an increase in initial susceptibility, but in a parallel texture it increased much more than in a perpendicular or random texture. It was assumed in [7] that nanoparticles are embedded at the nodes of a simple cubic lattice (Simple Cubic Lattice of Ferroparticles - SCLF) and the relaxation of the magnetic moments of nanoparticles occurs by the Brownian mechanism. The particles did not have their own magnetic anisotropy, but could rotate in the lattice nodes under the influence of an external magnetic field and as a result of interparticle dipole interactions. The magnetic properties of SCLF were compared with the magnetic properties of the ferrofluid modeled by the system of Dipole Hard Spheres (DHS). It has been established that the magnetizations of DHS and SCLF are the same for weak dipole-dipole interactions. With strong and moderate dipole coupling and a weak magnetic field, the DHS system is magnetized higher than the SCLF system, while with stronger fields, the opposite trend is observed. The article [7] discusses the reasons for such behavior.

Works [7, 17] demonstrate how different distributions of magnetic nanoparticles inside a sample can change its macroproperties. Nevertheless, the theory of dipole-dipole interactions in a system of stationary superparamagnetic particles remains incomplete. Unlike previous works, where only parallel and perpendicular cases of the arrangement of the easy axes relative to the external magnetic field were considered, in this work, using a statistical-mechanical approach, the thermodynamic and magnetic properties of an ensemble of the stationary monodisperse superparamagnetic particles located randomly at the nodes of a simple cubic lattice are analyzed, and their easy axes are aligned parallel to each other and located at an arbitrary angle to the external magnetic field.

2. Model

The sample under study is a monodisperse system of N fixed superparamagnetic spherical particles, which are affected by an external magnetic field. All particles have the same diameter of the magnetic core x and magnetic moment $m = v_m M_s$, where M_s — is the bulk saturation magnetization of the magnetic material, and $v_m = \pi x^3/6$ — is the volume of the magnetic core. The magnetic moment and the radius vector of the i-th particle are, respectively, $\mathbf{m}_i = m_i \boldsymbol{\Omega}_i$ and $\mathbf{r}_i = r_i \hat{\mathbf{r}}_i$, where $\boldsymbol{\Omega}_i = (\sin\omega_i \cos\xi_i, \sin\omega_i \sin\xi_i, \cos\omega_i)$ and $\hat{\mathbf{r}}_i = (\sin\tau_i \cos\phi_i, \sin\tau_i \sin\phi_i, \cos\tau_i)$ are the unit vectors. Each magnetic moment tends to be parallel or antiparallel to the easy axis, which determines two main positions. The direction of the applied magnetic field $\mathbf{H}$ is parallel to the Oz axis, that is, $\mathbf{H} = H\mathbf{h} = H(0,0,1)$. The sample has the shape of a cylinder, strongly elongated along the Oz axis. This form is used in order to avoid the occurrence of demagnetizing fields. It is assumed that all simple axes are parallel to each other and can be described by a single vector $\mathbf{n}$, which is determined by the angles θ and φ. The angle θ is the angle between the vectors $\mathbf{H}$ and $\mathbf{n}$: $\theta = \angle(\mathbf{H},\mathbf{n})$. The angle φ is the polar angle in the Oxy plane. The coordinate system, the direction of the external magnetic field, and the easy axis are illustrated in (Fig. 1.).

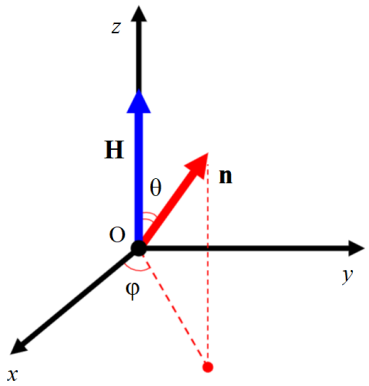

Fig. 1. The coordinate system; the Oz axis is parallel to the direction of the applied external magnetic field $\mathbf{H}$.

The Néel energy is given as a function depending on the angle between vector $\mathbf{n}$ and the magnetic moment $\mathbf{m}_i$:

$$U_N(i) = -Kv_m\left(\mathbf{\Omega_i}\cdot\hat{\mathbf{n}}\right)^2,$$

where $\hat{\mathbf{n}}$ — is the unit vector, and K — is the magnetic crystallographic anisotropy constant (characteristic of the material).

The Zeeman energy describes the interaction between the magnetic moment $\mathbf{m}_i$ and the homogeneous external magnetic field $\mathbf{H}$

$$U_m(i) = -\mu_0\left(\mathbf{m}_i\cdot\mathbf{H}\right) = -\mu_0 mH\cos\omega_i,$$

taking into account the strength and directivity of the applied magnetic field $\mathbf{H}$; μ_0 — – is the magnetic permeability of the medium.

The paired dipole-dipole interaction of the i - th and j - th particles is found using the anisotropic potential U_d:

$$U_d(ij) = \frac{\mu_0 m^2}{4\pi r_{ij}^3}\left[\left(\mathbf{\Omega}_i\cdot\mathbf{\Omega}_j\right) - 3\left(\mathbf{\Omega}_i\cdot\hat{\mathbf{r}}_{ij}\right)\left(\mathbf{\Omega}_j\cdot\hat{\mathbf{r}}_{ij}\right)\right],$$

where $\mathbf{r}_{ij} = r_{ij}\hat{\mathbf{r}}_{ij} = \mathbf{r}_j - \mathbf{r}_i$ denotes the vector with the length $r_{ij} = \left|\mathbf{r}_{ij}\right|$, connecting centers of the i - th and j - th particles.

The total potential energy, normalized to thermal energy (Boltzmann constant) $k_B T = \beta^{-1}$, is defined in the following form:

$$\beta U = \beta\sum_{j>i=1}^{N} U_d(ij) - \alpha\sum_{i=1}^{N}\left(\mathbf{\Omega}_i\cdot\hat{\mathbf{h}}\right) - \sigma\sum_{i=1}^{N}\left(\mathbf{\Omega_i}\cdot\hat{\mathbf{n}}\right)^2.$$

Here: $\alpha = \beta\mu_0 mH$ — is the Langevin parameter; $\sigma = \beta v_m K$ — is the dimensionless anisotropy parameter; $\hat{\mathbf{h}}$ — is the unit vector.

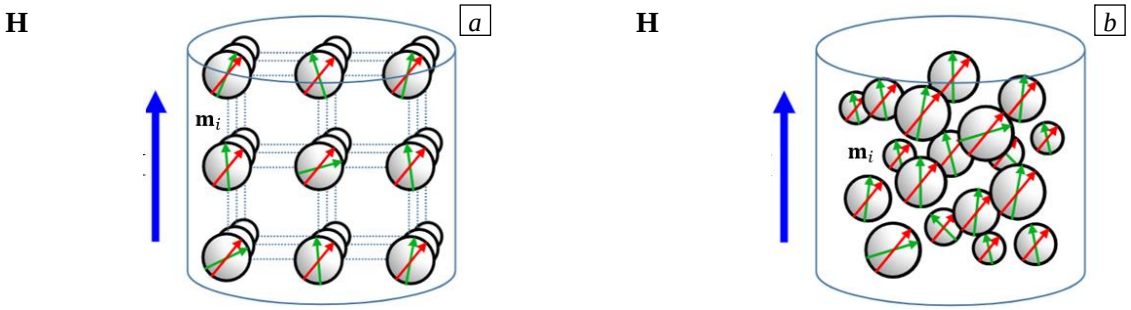

Fig. 2. A monodisperse system of stationary single-domain superparamagnetic ferroparticles in the external magnetic field $\mathbf{H}$: the distribution of the particles by volume is assumed at the nodes of a simple cubic lattice (a) or randomly (b).

The location of the particle at the point in the volume is described using the probability function, defined through the delta function: $p(\mathbf{r}_k) = \delta\left(\mathbf{r}_k - \mathbf{r}_k^{(0)}\right)$. Two types of particle volume distribution will be considered: at the nodes of the simple cubic lattice and randomly. Both textures of the particle distribution in the sample are shown in (Fig. 2).

For the more detailed description of the model and its magnetic susceptibility, we will use the standard parameter - the initial Langevin susceptibility:

$$\chi_L = \frac{4\pi\mu_0\rho m^2}{3k_B T},$$

where ρ — is the numerical concentration of the ferrocarticles in the sample.

3. Expansion of the Helmholtz free energy for an ensemble of stationary particles

To consider the magnetic and thermodynamic properties of the system, we will use a classical technique for a similar problem — the decomposition of the Helmholtz free energy F Let us write down the definition of F in terms of the configuration integral Z, which describes all deviations of the system from the ideal state:

$$\beta F = -\ln(Z).$$

In order to establish the contribution of the dipole-dipole interactions to the change in the parameters of the system, we represent F in the form of two terms:

$$F = F_{id} + \Delta F.$$

The first term F_{id} corresponds to an ideal thermodynamic system of non-interacting superparamagnetic nanoparticles in an applied magnetic field. The second term ΔF shows the contribution of dipole-dipole interactions to the Helmholtz free energy.

For convenience, we introduce the following notation: ΔF^{SCLF} and ΔF^{RANDOM} — the contribution of dipole-dipole interactions to the Helmholtz free energy for the case of a cubic lattice and a random distribution, respectively.

3.1. Ideal superparamagnetic system

The Helmholtz free energy for an ideal system of superparamagnetic non-interacting particles in the applied magnetic field — F_{id}, will take the following form:

$$\beta F_{id} = -\ln(Z_{id}),$$
$$Z_{id} = \prod_{k=1}^{N}\int p(\mathbf{r}_k)\exp\left(\sum_{i=1}^{N}\left[\exp\left[\alpha\cos\omega_i + \sigma\left(\mathbf{\Omega}_1\cdot\hat{\mathbf{n}}\right)^2\right]\right]\right)d\mathbf{r}_k d\mathbf{\Omega}_k \ . \qquad (1)$$

Here $d\mathbf{r}_k$ and $d\mathbf{\Omega}_k$ are averaging over all possible locations and directions of the magnetic moment of the k - th particle, respectively:

$$d\mathbf{r}_k = r_k^{\,2}\sin\theta_k dr_k d\theta_k d\varphi_k,$$
$$d\mathbf{\Omega}_k = \frac{1}{4\pi}\sin\omega_k dr_k d\omega_k d\xi_k;$$

$\mathbf{\Omega}_1$ — is the vector describing the direction of the magnetic moment.

As it can be seen from the definition (1), Z_{id} depends only on the single–particle interaction types: magnetic moment - magnetic field and magnetic moment - easy axis. This ideal case completely neglects the interparticle dipole-dipole interactions, which depend on the location of the particles in the sample volume. Taking into account the normalization rule for both the lattice and random distribution:

$$\int p(\mathbf{r}_k)\,d\mathbf{r}_k = 1,$$

it can be concluded that all the particles are equivalent to each other when integrating. This allows us to rewrite the expression for Z_{id} as:

$$Z_{id} = \left(\int \exp\left[\alpha \cos\omega_1 + \sigma \left(\mathbf{\Omega}_1 \cdot \hat{\mathbf{n}} \right)^2 \right] d\mathbf{\Omega}_1 \right)^N .$$

The result can be found numerically for the fixed direction of the vector $\hat{\mathbf{n}}_1$ and each set of the parameters α and σ. It should be noted that the configuration integral in the Helmholtz free energy for the ideal system will not be conditioned by the temperature and concentration of the particles:

$$\frac{\beta F_{id}}{N} = -\ln\left(\int \exp\left[\alpha \cos\omega_1 + \sigma \left(\mathbf{\Omega}_1 \cdot \hat{\mathbf{n}} \right)^2 \right] d\mathbf{\Omega}_1 \right). \quad (2)$$

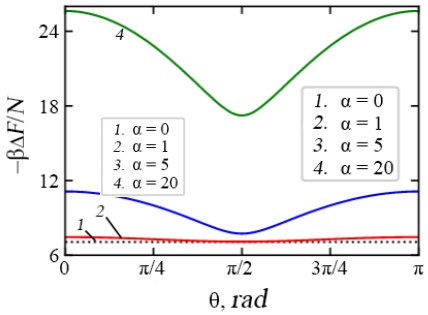

Fig. 3. Helmholtz free energy as the function depending on the angle $\theta = \angle(\mathbf{H}, \mathbf{n})$ for the ideal system of superparamagnetic particles with $\chi_L = 1{,}25$, $\sigma = 10$ and different value of the parameter α: 0 (curve *1*); 1 (*2*); 5 (*3*); 20 (*4*).

For the ideal case in the zero magnetic field, there is no dependence of the integral on the angle θ. Also, for any parameters there is no dependence on the angle φ. The system is completely isotropic when rotating in the Oxy plane.

Fig. 3 shows that with an increase in the strength of the external magnetic field a minimum appears at the point $\pi/2$ Parallel configurations of the energy curves, in which the anisotropy axis is located along the magnetic field vector ($\theta = 0$ and $\theta = \pi$), show faster growth of free energy than in the perpendicular configuration ($\theta = \pi/2$).

3.2. Dipole-dipole interaction

Consider the contribution of the dipole-dipole interactions to the Helmholtz free energy

$$\beta\Delta F = -\ln\left(\frac{Z}{Z_{id}} \right),$$

$$\frac{Z}{Z_{id}} = \frac{1}{Z_{id}} \prod_{k=1}^{N} \int p(\mathbf{r}_k) \exp\left(-\sum_{j>i=1}^{N} U_d(ij) + \sum_{i=1}^{N} \left[\exp\left[\alpha \cos\omega_i + \sigma \left(\mathbf{\Omega}_1 \cdot \hat{\mathbf{n}} \right)^2 \right] \right] \right) d\mathbf{r}_k d\mathbf{\Omega}_k .$$

Rewrite the last expression in the more compact form:

$$\frac{Z}{Z_{id}} = \prod_{k=1}^{N} \int p(\mathbf{r}_k) \prod_{j>i=1}^{N} \left(1 + f_{ij} \right) d\mathbf{r}_k d\Psi_k ,$$

where $f_{ij} = \left(\exp\left(-\beta U_d(ij) \right) - 1 \right)$ — is the Mayer function, and $d\Psi_k$ — is the Boltzmann averaging over the orientation of the magnetic moment of the k - th nanoparticle:

$$d\Psi_k = \frac{\exp\left[\alpha \cos\omega_k + \sigma \left(\mathbf{\Omega}_k \cdot \hat{\mathbf{n}} \right)^2 \right] d\mathbf{\Omega}_k}{\int \exp\left[\alpha \cos\omega_1 + \sigma \left(\mathbf{\Omega}_1 \cdot \hat{\mathbf{n}} \right)^2 \right] d\mathbf{\Omega}_1} .$$

Summarizing all the available data, it is possible to obtain the final form of the configuration part of the Helmholtz free energy and write the final expression for the simple cubic lattice:

$$\frac{\beta\Delta F^{SCLF}}{N} = -\frac{1}{2}\sum_{j=2}^{N} f_{1j}^{(0)}, \tag{3}$$

where $f_{1j}^{(0)} = \int p(\mathbf{r}_1)d\mathbf{r}_1 \int p(\mathbf{r}_j) f_{1j} d\mathbf{r}_j$ is the Mayer function for the 1-th and j-th nanoparticles located in the lattice and $\left\langle f_{1j}^{(0)} \right\rangle$ — is the Boltzmann averaging over the orientation of the magnetic moment of the 1-th and j-th nanoparticles:

$$\left\langle f_{1j}^{(0)} \right\rangle = \int f_{1j}^{(0)} d\Psi_1 d\Psi_j.$$

The definition of ΔF from (3) is valid for regular types of nanoparticle distribution in the system volume, such as SCLF or other lattices. For random placement of magnetic nanoparticles in the sample volume, it is necessary to average (3) over all possible random configurations. This means that, in the limit, each j- th particle in the sum (3) can occupy any position in the sample volume, except of the position of the 1-th particle:

$$\frac{\beta\Delta F^{RANDOM}}{N} = -\frac{1}{2}\sum_{j=2}^{N}\int \langle f_{1j} \rangle \frac{dr_{1j}}{V} = -\frac{N}{2V}\int \langle f_{12} \rangle dr_{12} = -\frac{\rho}{2}\int \langle f_{12} \rangle dr_{12}, \tag{4}$$

where $\rho = N/V$ — is the density of the distribution of the particles by the volume.

Decompose the Mayer function f_{ij} into a series up to terms with the second order of the dipole energy U_d inclusively:

$$f_{12} = -\beta U_d(12) + \frac{1}{2!}\left[-\beta U_d(12)\right]^2 + \mathrm{O}\left(U_d{}^3\right),$$
$$f_{1j}^{(0)} = -\beta U_d(1j) + \frac{1}{2!}\left[-\beta U_d(1j)\right]^2 + \mathrm{O}\left(U_d{}^3\right).$$

For the cubic lattice, the configurational part of the Helmholtz free energy (3) can be written as:

$$\frac{\beta\Delta F^{SCLF}}{N} \approx -\frac{1}{2}(b_1 + b_2),$$

where

$$b_1 = \sum_{j=2}^{N}\langle -\beta U_d(1j)\rangle, \quad b_2 = \frac{1}{2!}\sum_{j=2}^{N}\left\langle \left(-\beta U_d(1j)\right)^2 \right\rangle.$$

Averaging the coefficients b_1 and b_2 by the direction of the magnetic moment, we obtain the final expression for the ΔF^{SCLF} in the logarithmic form:

$$\frac{\beta\Delta F^{SCLF}}{N} = -\ln\left\{1 + 0,5\chi_L\left[Q_z^2 - 0,5Q_x^2 - 0,5Q_y^2\right] + \right.$$
$$\left. +0,5\chi_L^2\left[0,381\left(Q_{xx}^2 + Q_{yy}^2 + Q_{zz}^2\right) + 0,098\left(Q_{xx}Q_{yy} + Q_{xx}Q_{zz} + Q_{yy}Q_{zz}\right) - 0,282\left(Q_{xy}^2 + Q_{xz}^2 + Q_{yz}^2\right)\right]\right\}. \tag{5}$$

Similarly, we write the configuration part of the free energy Helmholtz for the random distribution (4):

$$\frac{\beta\Delta F^{RANDOM}}{N} \approx -\frac{\rho}{2}(b_1 + b_2),$$

where

$$b_1 = \int \langle -\beta U_d(12) \rangle d\mathbf{r}_{12}, \qquad b_2 = \frac{1}{2!}\int \left\langle \left(-\beta U_d(12)\right)^2 \right\rangle d\mathbf{r}_{12}.$$

Averaging the coefficients b_1 and b_2 by the direction of the magnetic moment, we obtain the final expression for the ΔF^{RANDOM} in the logarithmic form:

$$\frac{\beta \Delta F^{RANDOM}}{N} = -\ln\left\{1 + 0,5\chi_L\left[Q_z^2 - 0,5Q_x^2 - 0,5Q_y^2\right] + \right.$$
$$\left. +0,1\chi_L\lambda\left[2\left(Q_{xx}^2 + Q_{yy}^2 + Q_{zz}^2\right) + Q_{xy}^2 + Q_{xz}^2 + Q_{yz}^2 + 3\left(Q_{xx}Q_{yy} + Q_{xx}Q_{zz} + Q_{yy}Q_{zz}\right)\right]\right\}, \qquad (6)$$

where $\lambda = \left(\mu_0 m^2 \beta\right)/\left(4\pi d^3\right)$ — is the dimensionless parameter describing the intensity of the magnetic interaction of two particles in units of the thermal energy.

To simplify the final form of the record, the following auxiliary functions Q_x, Q_y, Q_z, Q_{xy}, Q_{xz}, Q_{yz}, Q_{xx}, Q_{yy} and Q_{zz} were used, which have the form:

$$Q_x(\alpha,\sigma,\hat{\mathbf{n}}) = \int \sin\omega_1 \cos\xi_1 d\Psi_1,$$
$$Q_y(\alpha,\sigma,\hat{\mathbf{n}}) = \int \sin\omega_1 \sin\xi_1 d\Psi_1,$$
$$Q_z(\alpha,\sigma,\hat{\mathbf{n}}) = \int \cos\omega_1 d\Psi_1,$$
$$Q_{xy}(\alpha,\sigma,\hat{\mathbf{n}}) = \int \sin^2\omega_1 \sin\xi_1 \cos\xi_1 d\Psi_1,$$
$$Q_{xz}(\alpha,\sigma,\hat{\mathbf{n}}) = \int \sin\omega_1 \cos\omega_1 \cos\xi_1 d\Psi_1,$$
$$Q_{zy}(\alpha,\sigma,\hat{\mathbf{n}}) = \int \sin\omega_1 \cos\omega_1 \sin\xi_1 d\Psi_1,$$
$$Q_{xx}(\alpha,\sigma,\hat{\mathbf{n}}) = \int \sin^2\omega_1 \cos^2\xi_1 d\Psi_1,$$
$$Q_{yy}(\alpha,\sigma,\hat{\mathbf{n}}) = \int \sin^2\omega_1 \sin^2\xi_1 d\Psi_1,$$
$$Q_{zz}(\alpha,\sigma,\hat{\mathbf{n}}) = \int \cos^2\omega_1 d\Psi_1.$$

3.3. Comparison of the results

Note that the first terms on the right side of the expressions (5) and (6), containing the magnetic energy of the interaction of the particles of the first order, coincide in form. Theoretical consideration of the differences in the structures of the spatial arrangement of the particles is possible only with an increase in the order of this energy. Expression (5) contains the full square of the Langevin's susceptibility χ_L^2, while expression (6) includes the product $\chi_L\lambda$. It is impossible to find unambiguously the parameter λ by setting only the value of the Langevin's susceptibility. Therefore, for definiteness, we choose the value λ based on the condition: $\chi_L\lambda = \chi_L^2$, that is, we assume that $\lambda = \chi_L$. Such restriction is introduced in order to compare two different expressions of the free energy corresponding to the two different models of particle placement in a sample on a particular example.

The ratio $\lambda = \chi_L$ is valid for the system with the fixed volume concentration of particles $\rho v_0 = 0,125$, which corresponds to the sample with a moderate concentration and should not lead to any unexpected effects. Let us trace the behavior of ΔF for the lattice and the random distribution by fixing $\chi_L = 1,25$, which will allow us to consider a wide range of anisotropy parameters. Let us put $\lambda = 1,25$ and $\sigma = 10$.

When analyzing the graphs of the ΔF for the lattice as the function of the azimuth angle θ (Fig. 4), we can notice that for all parameters there are always two minima. There is also a clear dependence on the angle φ. In this case, the graph for $\varphi = \pi/3$ coincides with the graph for $\varphi = \pi/6$, and the graph for $\varphi = \pi/2$ — coincides with the graph $\varphi = 0$. As a result, additional cases $\varphi = \pi/3$ and $\varphi = \pi/2$ are not shown in the figure.

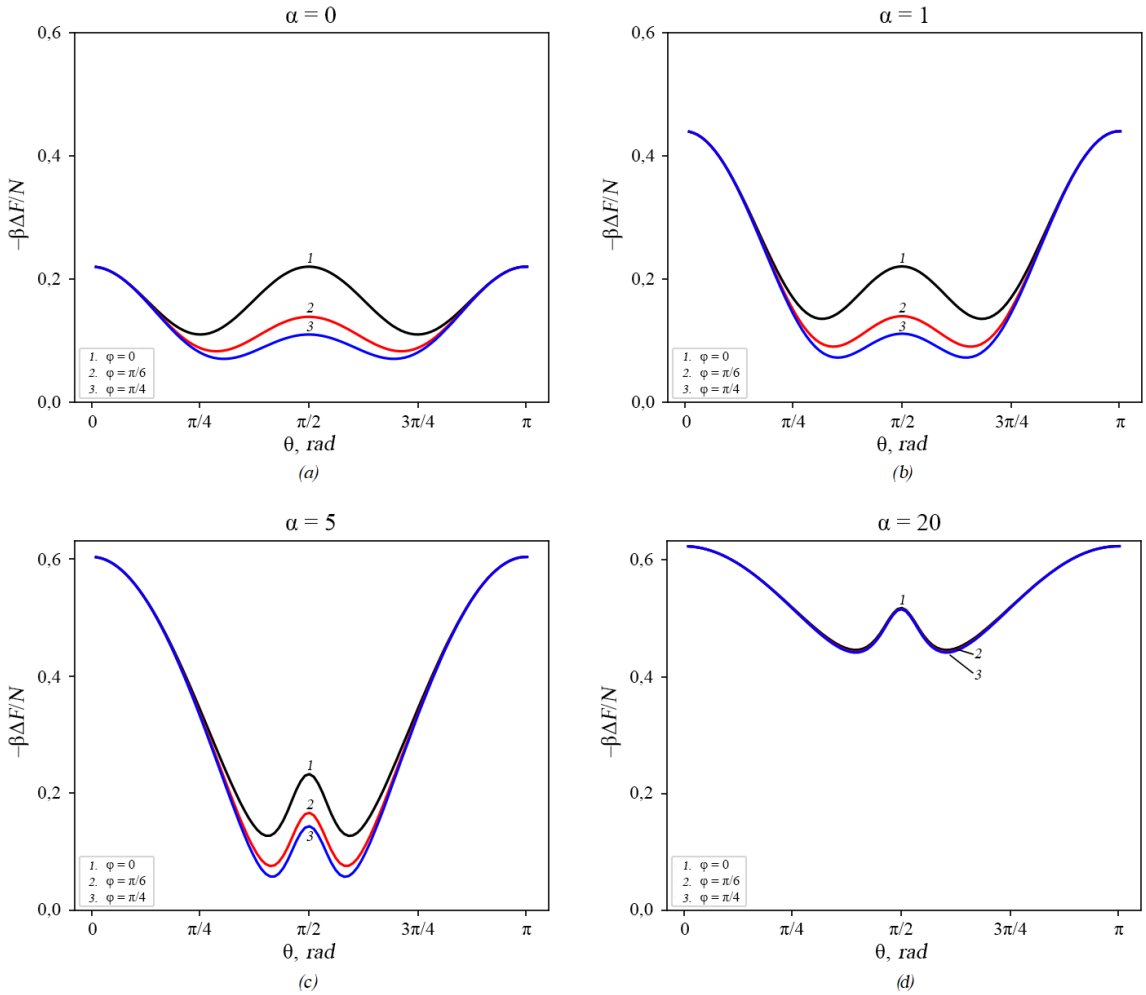

Fig. 4. The contribution of the dipole-dipole interactions: ΔF as a function, which depends on the angle $\theta = \angle(\mathbf{H},\mathbf{n})$, for the cubic lattice with $\chi_L = 1{,}25$, $\sigma = 10$ and different values of the external magnetic field: $\alpha = 0$ (a); $\alpha = 1$ (b); $\alpha = 5$ (c); $\alpha = 20$ (d).

In the case of a zero magnetic field (see Fig. 4a) for $\varphi = 0$, three maxima are located at the same level. The physical reason for the two minima at the points $\theta = \pi/4$ and at $\theta = 3\pi/4$ for $\varphi = 0$ is that at these angle values, the dipoles in the head-tail orientation are located diagonally across the spatial lattice, which means that the distance between the dipoles will be maximum. This leads to a decrease in the energy of their interaction. As the angle φ increases from 0 to $\pi/4$, the dipoles move away from each other, and as a result, the average maximum shifts down relative to right and left maxima. (Fig.4b) shows that the appearance of an external magnetic field of low intensity noticeably increases the frequency of dipole-dipole interactions only for parallel configurations at $\theta = 0$ and $\theta = \pi$. The maximum at the point $\theta = \pi/2$ practically does not move upwards, but at the same time, two minima are shifted to this point. All the features noted in the previous case, appear more pronounced with an increase in the external magnetic field (see Fig. 4c). For strong magnetic fields shown in (Fig. 4d), corresponding to the state of magnetic saturation of the system, the sensitivity to the magnitude of the angle φ disappears, and there is also a vertical upward shift of the average local maximum and two minima, which was not observed in previous cases.

Considering the graphs ΔF for the random distribution as a function of the azimuth angle θ (Fig. 5), we can come to the following conclusions: there is no dependence on the angle φ for any parameters ΔF. The system is completely isotropic when rotating in the Oxy plane. As in the ideal case, there is no dependence on the angle θ in a zero magnetic field. With an increase in the strength of the external magnetic field, two minima appear, which approach to $\theta = \pi/2$ with an increase in the parameter α. The parallel configurations in which the anisotropy axis is located along the magnetic field vector, that is $\theta = 0$ and $\theta = \pi$, show a faster growth of ΔF, than the perpendicular configuration $\theta = \pi/2$. With the strengthening of the field, there is not

only a vertical upward movement of the graph, but also the increase in the height of its deflection. In the strong magnetic field ($\alpha = 20$), in the state of magnetic saturation of the system, there is a vertical shift of the average local maximum and two minima upward, which is missing for $\alpha = 1$ and $\alpha = 5$, and the contribution of dipole-dipole interactions to the free energy for the parallel configurations practically does not change in comparison with the state in the field $\alpha = 5$.

Summarizing the results obtained for the cubic lattice and random distribution, we can draw the following conclusions:

– the state of magnetic saturation does not depend on the angle φ; the difference between the two types of the sample texture is depending on the angle φ in all cases, except for the state of the magnetic saturation; the random distribution is completely isotropic when rotated in the Oxy plane;

– in a zero magnetic field ΔF for the cubic lattice depends on the angle θ, while there is no such dependence for the random distribution;

– for both textures, the graphs have similar character with two minima and three maxima for parallel ($\theta = \pi/4$ и $\theta = \pi$) and perpendicular ($\theta = \pi/2$)vectors.

4. Results

4.1. Initial magnetic susceptibility

The initial magnetic susceptibility was calculated using the analytical expression of the Helmholtz free energy:

$$\chi = \chi_{id} - \frac{1}{V}\frac{\partial^2 \Delta F}{\partial H^2}\bigg|_{H=0},$$

where χ_{id} means the initial magnetic susceptibility of the ideal system without dipole-dipole interaction:

$$\chi_{id} = -\frac{1}{V}\frac{\partial^2 F_{id}}{\partial H^2}\bigg|_{H=0}.$$

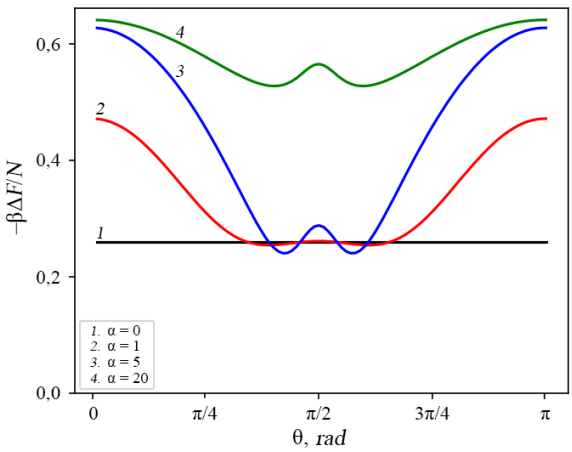

Fig. 5. The contribution of the dipole-dipole interactions: ΔF as a function depending on the angle $\theta = \angle(\mathbf{H}, \mathbf{n})$ for the random distribution with $\chi_L = 1{,}25$, $\sigma = 10$ and different values of the external magnetic field α: 0 (curve *1*); 1 (*2*); 5 (*3*); 20 (*4*).

Fig. 6 shows graphs of the initial magnetic susceptibility as a function depending on the angle θ, for the lattice — χ_{SCLF}, and the random structure — χ_{random}. As we can see, susceptibility reaches its minimum in the case of the perpendicular position of the easy axes relative to the external magnetic field, that is, when $\theta = \pi/2$. Such behavior is observed for both cubic and random distribution of the ferroparticles. But when their positions change from perpendicular to parallel, changes in the behavior of the graphs become noticeable: for random distribution, the growth of the initial magnetic susceptibility occurs more sharply, while for the cubic lattice it is smooth.

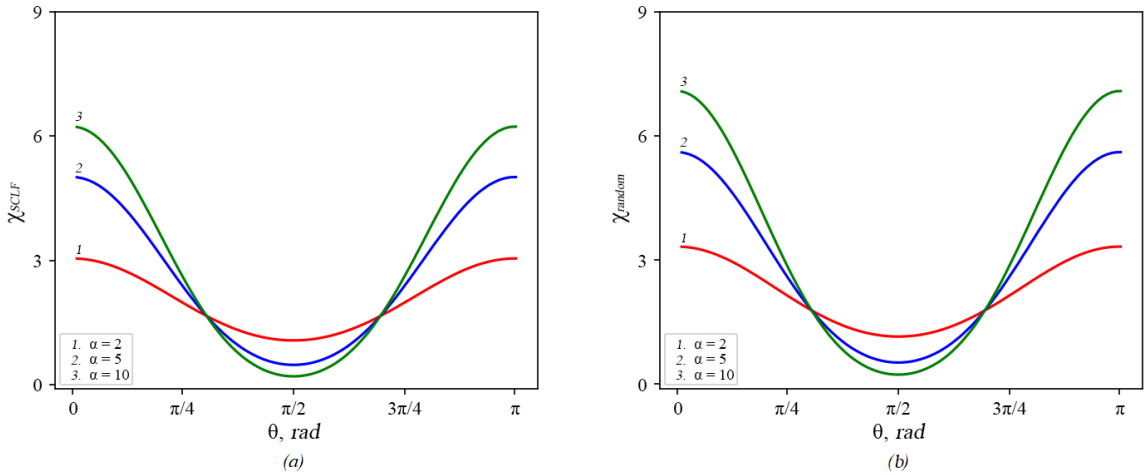

Fig. 6. The initial magnetic susceptibility as a function depending on the angle $\theta = \angle(\mathbf{H},\mathbf{n})$, for the cubic lattice (a) and random distribution (b) for the different values of the anisotropy parameter σ: 2 (curve *1*); 5 (*2*); 10 (*3*).

4.2. Static magnetization

The analytical form of scalar magnetization can be similarly obtained through the free Helmholtz energy:

$$M = M_{id} - \frac{\partial}{\partial\alpha}\left(\frac{\beta\Delta F}{N}\right),$$

where

$$M_{id} = -\frac{\partial}{\partial\alpha}\left(\frac{\beta F_{id}}{N}\right).$$

The expression for ΔF in the magnetization formula can be simplified by discarding some of the terms. Thus, in relations (3) and (4), only the functions Q_z, Q_{xx}, Q_{yy} and Q_{zz}, should be taken into account, since only they will give a non-zero contribution in the external magnetic field:

$$Q_z(\sigma=0) = L(\alpha),$$
$$Q_{xx}(\sigma=0) = Q_{yy}(\sigma=0) = \frac{L(\alpha)}{\alpha},$$
$$Q_{zz}(\sigma=0) = 1 - 2\frac{L(\alpha)}{\alpha},$$

when the remaining terms Q_x, Q_y, Q_{xy}, Q_{xz} and Q_{yz} will be zero at $\sigma = 0$.

(Fig. 7) shows graphs of static magnetization as a function depending on the angle θ, for the lattice (M_{SCLF}) and a random structure (M_{random}), respectively. As can be seen, in the weak field ($\alpha = 1$) the contribution of dipole-dipole interactions is especially noticeable.

With an increase in the field strength ($\alpha \geq 5$), the magnetic moments are aligned along the field and no longer show such a pronounced influence on each other.

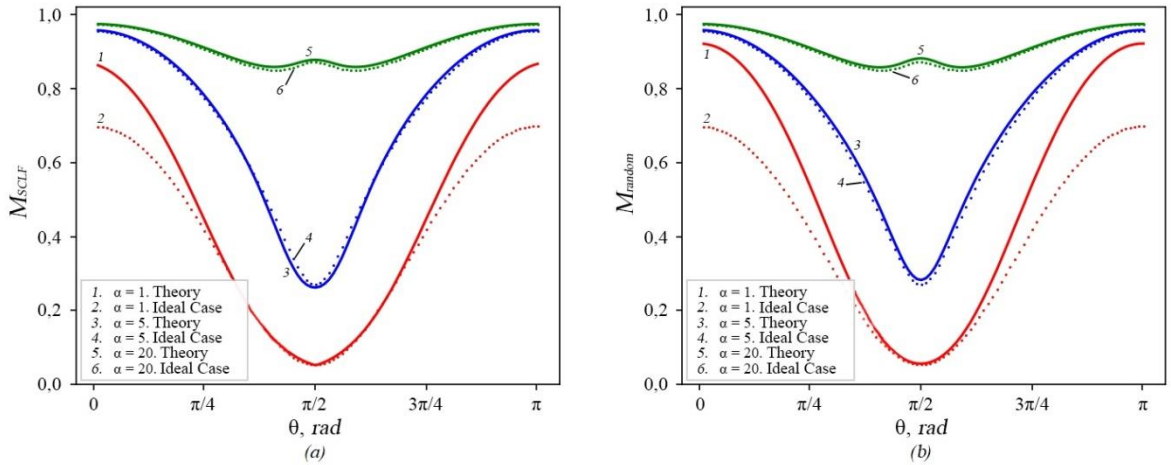

Fig. 7. The static magnetization M as a function depending on the angle $\theta = \angle(\mathbf{H},\mathbf{n})$, for the cubic lattice (a) and the random distribution (b) with $\chi_L = 1{,}25$, $\sigma = 10$ and different values of the external magnetic field α: 1 (curve *1*); 5 (*3*) and 20 (*5*); dotted curves *2*, *4*, *6* correspond to the ideal system.

4.3. Heat capacity

The formula for the heat capacity expressed in terms of the configuration integral looks as follows:

$$C_V = \frac{\partial}{\partial T}\left(k_B T^2 \frac{\partial \ln(Z)}{\partial T}\right).$$

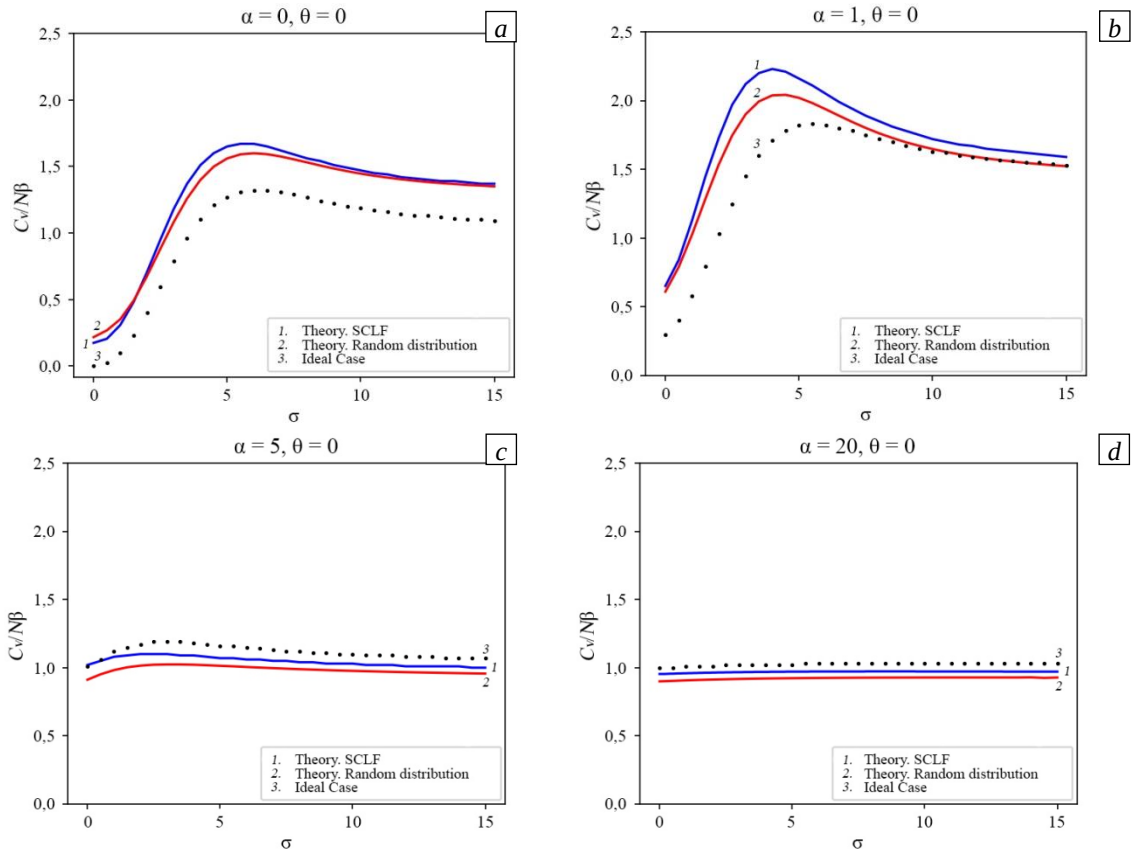

Fig. 8. The heat capacity C_V as a function depending on the anisotropy parameter σ, for the cubic lattice and random distribution with $\chi_L = 1{,}25$, $\theta = 0$ and various values of the external magnetic field α: 0 (a), 1 (b), 5 (c), 20 (d).

Let us write it down as:

$$C_V = k_B\left[\chi_L{}^2\frac{\partial^2 \ln(Z)}{\partial \chi_L{}^2}+\alpha^2\frac{\partial^2 \ln(Z)}{\partial \alpha^2}+\sigma^2\frac{\partial^2 \ln(Z)}{\partial \sigma^2}+2\chi_L\alpha\frac{\partial}{\partial \chi_L}\left(\frac{\partial \ln(Z)}{\partial \alpha}\right)+2\chi_L\sigma\frac{\partial}{\partial \chi_L}\left(\frac{\partial \ln(Z)}{\partial \sigma}\right)+2\alpha\sigma\frac{\partial}{\partial \alpha}\left(\frac{\partial \ln(Z)}{\partial \sigma}\right)\right].$$

Looking at formulas (1), (4) and (5), we can conclude that $\ln(Z)\sim F\sim N$, therefore, when considering the heat capacity graphs, we use the construction $C_V/(Nk_B)$.

(Fig. 8) and (Fig. 9) show graphs of the heat capacity as a function of the anisotropy parameter σ for the cubic lattice and the random distribution at different values of the external magnetic field α, in parallel ($\theta=0$) and perpendicular ($\theta=\pi/2$) positions of the easy axes relative to the external magnetic field. As can be seen from the graphs, for a strong field ($\alpha=20$) the proposed approach gives results that almost coincide with the ideal case, while with a weak field or its complete absence, the contribution of the dipole-dipole interactions becomes much more noticeable.

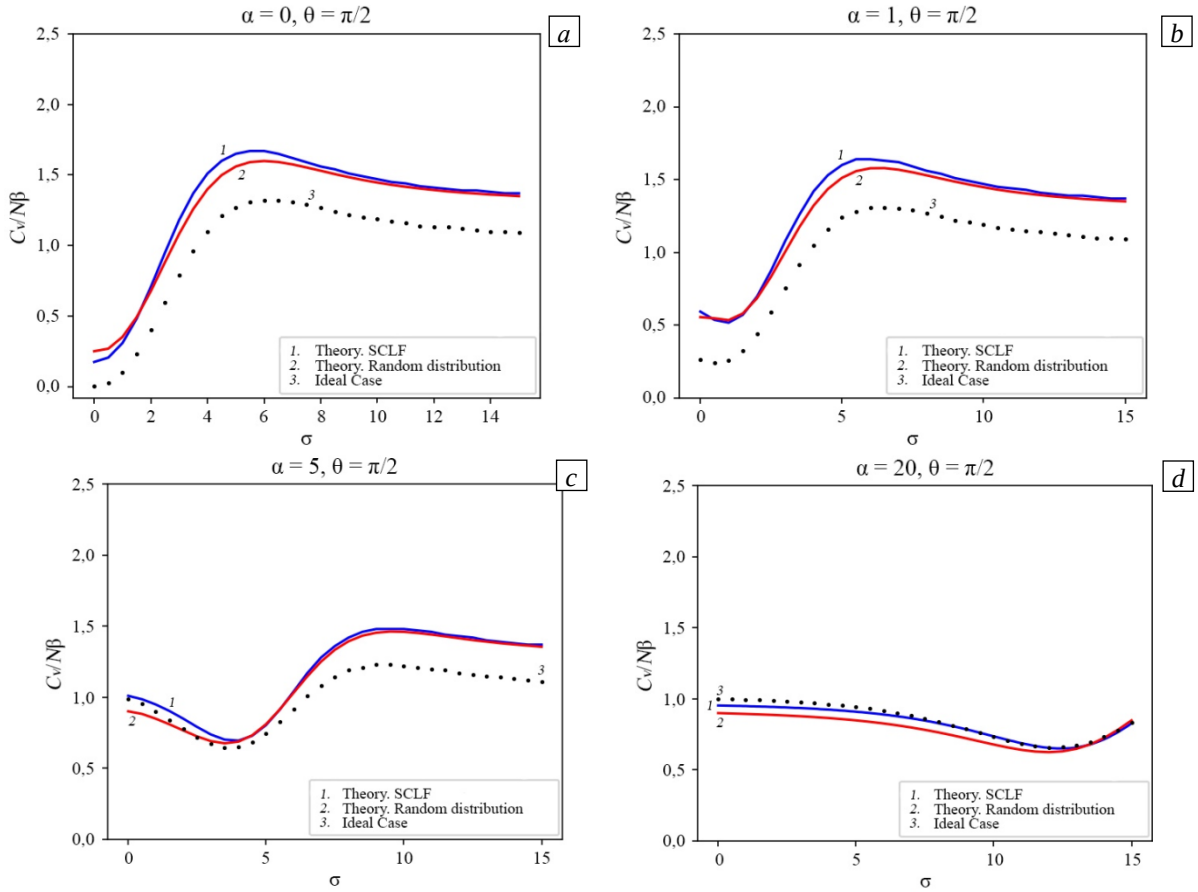

Рис. 9. The heat capacity C_V as a function depending on the anisotropy parameter σ, for the cubic lattice and random distribution with $\chi_L=1{,}25$, $\theta=\pi/2$ and various values of the external magnetic field α: 0 (a), 1 (b), 5 (c), 20 (d).

5. Conclusion

In contrast to previous works devoted to this topic, where only the perpendicular and parallel cases of the mutual arrangement of the easy axes and the external magnetic field were discussed, in this paper, using the statistical-mechanical approach, a more general case of an arbitrary angle is considered. The previously studied special cases follow from this theory, which confirms its generality. In addition, a comparative analysis of the behavior of the system for the cubic lattice and the random configurations was conducted. Using the generalized theory, the analysis of the static, magnetic, and thermodynamic properties of a system of stationary superparamagnetic particles in an external magnetic field is carried out for an arbitrary angle between the easy magnetization axes of the particles and the external magnetic field. The potential energy of the system included single-particle dipole-axial interaction, single-particle dipole-field interaction, and long-range interparticle

dipole-dipole correlations. Two types of arrangement of particles in the system are studied: at the nodes of the cubic lattice and randomly. For both textures, a theoretical expression for the Helmholtz free energy is obtained in logarithmic form. In developing the theory of dipole-dipole interactions in a system of stationary superparamagnetic particles, the decomposition of the Helmholtz free energy into the classical virial series was used. This approach has a number of disadvantages, for example, the alternation of the series and slow convergence. To weaken these effects, the work resorted to the logarithmic transformation of free energy, so that the final function in the form of a logarithm turns out to be less sensitive to the limitation of the number of terms in the series, and makes it possible to expand the applicability area of the developed theory to moderate densities of nanoparticles in the sample. On the basis of the obtained formulas for the Helmholtz free energy, a certain range of properties of the ferroparticle system has been studied: initial magnetic susceptibility, static magnetization, heat capacity. A graphical visualization is built for each parameter. It has been established that in a zero magnetic field the contribution of the dipole-dipole interparticle interaction to the Helmholtz free energy for an ordered system of particles depends on the polar angle φ, and when they are randomly placed in the volume, there is no such dependence. When analyzing the results, it turned out that the random distribution is completely isotropic when the particles rotate in the Oxy plane. It is also found that the state of magnetic saturation does not depend on the angle φ, and in a zero magnetic field there is no dependence on the angle θ for ΔF with the random distribution, while a similar conditionality is observed for the cubic lattice.

The author expresses his deep gratitude to his colleagues A.Y. Solovieva and E.A. Elfimova for their recommendations during the work on the manuscript of this article.

The study was supported by the Ministry of Science and Higher Education of the Russian Federation within the framework of the Ural Mathematical Center project No. 075-02-2021-1387.

References

1. Socoliuc V., Popescu L.B. Determination of the statistics of magnetically induced particle chains in concentrated ferrofluids. *J. Magn. Magn. Mater.*, 2020, vol. 502, 166532. https://doi.org/10.1016/j.jmmm.2020.166532
2. Elkady A.S., Iskakova L., Zubarev A. On the self-assembly of net-like nanostructures in ferrofluids. *Phys. Stat. Mech. Appl.*, 2015, vol. 428, pp. 257-265. https://doi.org/10.1016/j.physa.2015.01.053
3. Pshenichnikov A.F., Ivanov A.S. Magnetophoresis of particles and aggregates in concentrated magnetic fluids. *Phys. Rev. E*, 2012, vol. 86, 051401. https://doi.org/10.1103/PhysRevE.86.051401
4. Daffé N., Zečević J., Trohidou K.N., Sikora M., Rovezzi M., Carvallo C., Vasilakaki M., Neveu S., Meeldijk J.D., Bouldi N., Gavrilov V., Guyodo Y., Choueikani F., Dupuis V., Taverna D., Sainctavit P., Juhin A. Bad neighbour, good neighbour: how magnetic dipole interactions between soft and hard ferrimagnetic nanoparticles affect macroscopic magnetic properties in ferrofluids. *Nanoscale*, 2020, vol. 12, pp. 11222-11231. https://doi.org/10.1039/D0NR02023K
5. Ilg P. Equilibrium magnetization and magnetization relaxation of multicore magnetic nanoparticles. *Phys. Rev. B*, 2017, vol. 95, 214427. https://doi.org/10.1103/PhysRevB.95.214427
6. Pshenichnikov A.F., Kuznetsov A.A. Self-organization of magnetic moments in dipolar chains with restricted degrees of freedom. *Phys. Rev. E*, 2015, vol. 92, 042303. https://doi.org/10.1103/PhysRevE.92.042303
7. Solovyova A.Yu., Kuznetsov A.A., Elfimova E.A. Interparticle correlations in the simple cubic lattice of ferroparticles: Theory and computer simulations. *Phys. Stat. Mech. Appl.*, 2020, vol. 558, 124923. https://doi.org/10.1016/j.physa.2020.124923
8. Elfimova E.A., Ivanov A.O., Popescu L.B., Socoliuc V. Transverse magneto-optical anisotropy in bidisperse ferrofluids with long range particle correlations. *J. Magn. Magn. Mater.*, 2017, vol. 431, pp. 54-58. https://doi.org/10.1016/j.jmmm.2016.09.051
9. Ivanov A.O., Camp P.J. Theory of the dynamic magnetic susceptibility of ferrofluids. *Phys. Rev. E*, 2018, vol. 98, 050602. https://doi.org/10.1103/PhysRevE.98.050602
10. Solovyova A.Yu., Elfimova E.A., Ivanov A.O., Camp P.J. Modified mean-field theory of the magnetic properties of concentrated, high-susceptibility, polydisperse ferrofluids. *Phys. Rev. E*, 2017, vol. 96, 052609. https://doi.org/10.1103/PhysRevE.96.052609
11. Minina E.S., Blaak R., Kantorovich S.S. Pressure and compressibility factor of bidisperse magnetic fluids. *J. Phys.: Condens. Matter*, 2018, vol. 30, 145101. https://doi.org/10.1088/1361-648X/aab137

12. Szalai I., Nagy S., Dietrich S. Comparison between theory and simulations for the magnetization and the susceptibility of polydisperse ferrofluids. *J. Phys.: Condens. Matter*, 2013, vol. 25, 465108. https://doi.org/10.1088/0953-8984/25/46/465108
13. Nagornyi A.V., Socoliuc V., Petrenko V.I., Almasy L., Ivankov O.I., Avdeev M.V., Bulavin L.A., Vekas L. Structural characterization of concentrated aqueous ferrofluids. *J. Magn. Magn. Mater.*, 2020, vol. 501, 166445. https://doi.org/10.1016/j.jmmm.2020.166445
14. Lebedev A.V., Stepanov V.I., Kuznetsov A.A., Ivanov A.O., Pshenichnikov A.F. Dynamic susceptibility of a concentrated ferrofluid: The role of interparticle interactions. *Phys. Rev. E*, 2019, vol. 100, 032605. https://doi.org/10.1103/PhysRevE.100.032605
15. Linke J.M., Odenbach S. Anisotropy of the magnetoviscous effect in a ferrofluid with weakly interacting magnetite nanoparticles. *J. Phys.: Condens. Matter*, 2015, vol. 27, 176001. https://doi.org/10.1088/0953-8984/27/17/176001
16. Pousaneh F., de Wijn A.S. Kinetic theory and shear viscosity of dense dipolar hard sphere liquids. *Phys. Rev. Lett.*, 2020, vol. 124, 218004. https://doi.org/10.1103/PhysRevLett.124.218004
17. Elfimova E.A., Ivanov A.O., Camp P.J. Static magnetization of immobilized, weakly interacting, superparamagnetic nanoparticles. *Nanoscale*, 2019, vol. 11, pp. 21834-21846. https://doi.org/10.1039/C9NR07425B
18. Balescu R. *Equilibrium and nonequilibrium statistical mechanics*. John Wiley and Sons, 1975. 756 p.
19. Joslin C.G. The third dielectric and pressure virial coefficients of dipolar hard sphere fluids. *Mol. Phys.*, 1981, vol. 42, pp. 1507-1518.
20. Wertheim M.S. Exact solution of the mean spherical model for fluids of hard spheres with permanent electric dipole moments. *J. Chem. Phys.*, 1971, vol. 55, pp. 4291-4298. https://doi.org/10.1063/1.1676751
21. Kalikmanov V.I. Statistical thermodynamics of ferrofluids. *Phys. Stat. Mech. Appl.*, 1992, vol. 183, pp. 25-50. https://doi.org/10.1016/0378-4371(92)90176-Q
22. Buyevich Yu.A., Ivanov A.O., Zubarev A.Yu. Statistical thermodynamics of ferrocolloids. *J. Magn. Magn. Mater.*, 1990, vol. 85, pp. 33-36. https://doi.org/10.1016/0304-8853(90)90011-E

The authors declare no conflict of interests.
The paper was received on 14.04.2021.
The paper was accepted for publication on 07.06.2021.